iScience

CellPress
OPEN ACCESS

Article

Haemolysins are essential to the pathogenicity of deep-sea *Vibrio fluvialis*

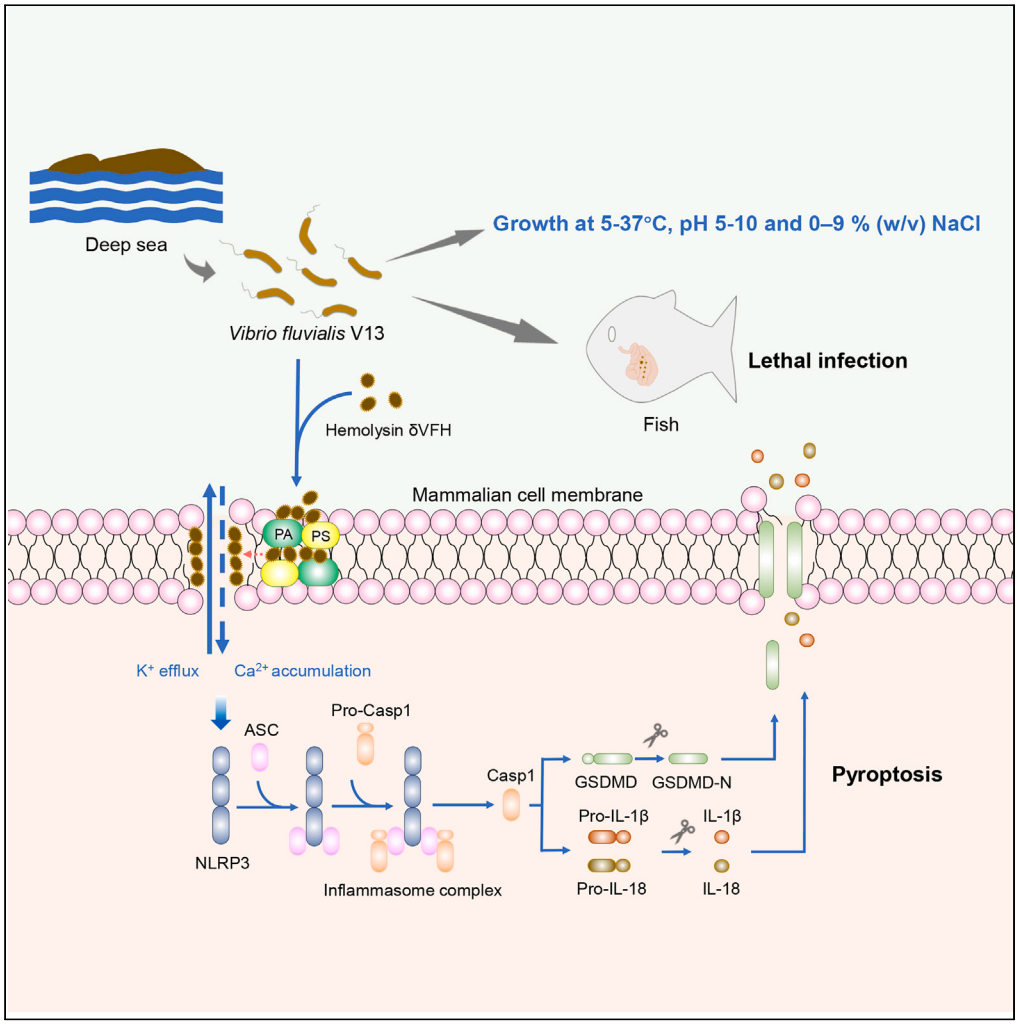

Yujian Wang, Jingchang Luo, Yan Zhao, Jian Zhang, Xiaolu Guan, Li Sun

zhaoyan1316@163.com (Y.Z.)
lsun@qdio.ac.cn (L.S.)

Highlights

The deep-sea isolate V13 caused lethal infection in fish and induced pyroptosis

The δVFH of V13 induced pyroptosis in a NLRP3-, K^+-, and Ca^{2+}- dependent manner

δVFH interactions with plasma membrane lipids were critical for pyroptosis induction

Wang et al., iScience 27, 109558
May 17, 2024
https://doi.org/10.1016/j.isci.2024.109558

iScience

CellPress
OPEN ACCESS

Article

Haemolysins are essential to the pathogenicity of deep-sea *Vibrio fluvialis*

Yujian Wang,[1,2,6] Jingchang Luo,[1,2,3,6] Yan Zhao,[4,6,*] Jian Zhang,[5] Xiaolu Guan,[1,2] and Li Sun[1,2,3,7,*]

SUMMARY

***Vibrio fluvialis* is an emerging foodborne pathogen that produces VFH (*Vibrio fluvialis* hemolysin) and δVFH (delta-*Vibrio fluvialis* hemolysin). The function of δVFH is unclear. Currently, no pathogenic *V. fluvialis* from deep sea has been reported. In this work, a deep-sea *V. fluvialis* isolate (V13) was examined for pathogenicity. V13 was most closely related to *V. fluvialis* ATCC 33809, a human isolate, but possessed 262 unique genes. V13 caused lethal infection in fish and induced pyroptosis involving activation of the NLRP3 inflammasome, caspase 1 (Casp1), and gasdermin D (GSDMD). V13 defective in VFH or VFH plus δVFH exhibited significantly weakened cytotoxicity. Recombinant δVFH induced NLRP3-Casp1-GSDMD-mediated pyroptosis in a manner that depended on K^+ efflux and intracellular Ca^{2+} accumulation. δVFH bound several plasma membrane lipids, and these bindings were crucial for δVFH cytotoxicity. Together these results provided new insights into the function of δVFH and the virulence mechanism of *V. fluvialis*.**

INTRODUCTION

Vibrio is a large genus of gram-negative bacteria and contains more than 100 known species.[1] Members of this genus are natural inhabitants of aquatic environments and prefer warm, brackish water, such as seawater.[1,2] Seawater is the ecological niche to many pathogenic microorganisms, including the vibrios.[3] Currently, at least 12 species of *Vibrio*, notably *Vibrio cholerae* and *Vibrio parahaemolyticus*, are known to cause human diseases in varying degrees, including gastrointestinal diseases, bacteremia, and septicemia.[1,3,4] *Vibrio* infection in humans occurs mainly via two transmission routes: contaminated water and unprocessed seafood.[5–7] In addition to be a human pathogen, some *Vibrio* species, such as *Vibrio anguillarum* and *Vibrio harveyi*, are notorious pathogens to a wide range of freshwater and marine animals.

Vibrio fluvialis was first isolated from diarrhea patients in Bangladesh during 1970s. Now it has become one of the emerging foodborne pathogens of the *Vibrio* genus. *V. fluvialis* outbreaks have been reported worldwide, often in association with poor conditions of sanitation and consumption of *V. fluvialis*-contaminated seafoods. *V. fluvialis* infection leads to acute gastroenteritis as well as other diseases.[8] Two reports showed that *V. fluvialis* exhibited distinct cytotoxic effects on HeLa cells and Chinese hamster ovary cells.[9,10] Similar to *V. cholerae* and *V. parahaemolyticus*, which are known to produce disease-inducing toxins,[11–13] *V. fluvialis* also produces a variety of toxins, including the heat-labile cytotoxin VFH (*Vibrio fluvialis* hemolysin) and thermostable hemolysins, such as delta-*Vibrio parahaemolyticus* hemolysin-like hemolysin, TDH (thermostable direct hemolysin), and TRH (TDH related hemolysin).[14–17] Two studies showed that VFH was able to lyse the erythrocytes of various animal species and played a critical role in the activation of the NLRP3 inflammasome during *V. fluvialis* infection.[10,18] In contrast, for the thermostable hemolysins, although they have long been known to be the key virulence factors of *V. parahaemolyticus*,[19–21] the role of these toxins in *V. fluvialis* remains to be studied.

Hydrothermal vents are the most spectacular ecological structures in the deep-sea. They provide habitats for diverse bacteria and archaea, which utilize the various hydrocarbon compounds, such as hydrogen sulfide, produced by the hydrothermal activity as energy sources.[22,23] *Vibrio* spp., such as *Vibrio harveyi* and *Vibrio diabolicus*, have been reported to exist in deep-sea hydrothermal vents, and some vibrios, such as *Vibrio antiquaries* and *Vibrio bathopelagicus*, possess virulence potentials.[24–26] To date, reports on deep-sea *V. fluvialis* are very limited and mainly focus on the function of metabolites and environmental adaptation.[27,28] To our knowledge, no study on the pathogenicity of deep-sea *V. fluvialis* has been documented. In the present work, we investigated the infectivity and virulence mechanism of V13, a *V. fluvialis* isolate from a deep-sea hydrothermal vent. We found that V13 was pathogenic and induced pyroptotic death of human cells. We further

[1]CAS and Shandong Province Key Laboratory of Experimental Marine Biology, Institute of Oceanology, Center for Ocean Mega-Science, Chinese Academy of Sciences, Qingdao, China
[2]Laboratory for Marine Biology and Biotechnology, Qingdao Marine Science and Technology Center, Qingdao 266237, China
[3]College of Marine Sciences, University of Chinese Academy of Sciences, Beijing 100049, China
[4]Tsinghua-Peking Joint Center for Life Sciences, School of Medicine, Tsinghua University, Beijing 100084, China
[5]School of Ocean, Yantai University, Yantai 264005, China
[6]These authors contributed equally
[7]Lead contact
*Correspondence: zhaoyan1316@163.com (Y.Z.), lsun@qdio.ac.cn (L.S.)
https://doi.org/10.1016/j.isci.2024.109558

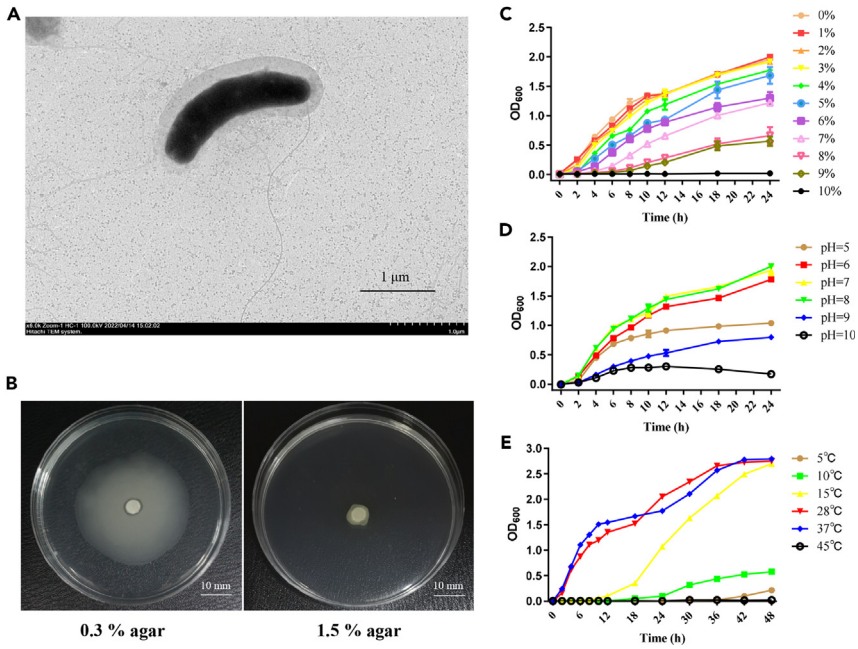

Figure 1. The morphology and growth of V13

(A) The image of V13 observed with a transmission electron microscope.

(B) The growth of V13 in marine 2216E containing 0.3% (left) and 1.5% (right) agar.

(C–E) The growth of V13 at different NaCl concentrations (C), pH levels (D), and temperature (E). The results are the means of triplicate experiments and shown as means ± standard deviation (SD).

examined the cytotoxicity of V13 hemolysins and demonstrated that the thermostable hemolysin δVFH (delta-*Vibrio fluvialis* hemolysin), as well as VFH, played an important role in the virulence of V13. These results provided new insights into the pathogenic mechanism of *V. fluvialis*.

RESULTS

The basic biological features of V13

The genome of V13 was sequenced, which showed that V13 contained two circular chromosomes of 3,132,683 and 1,653,670 bp, respectively, and 50.16% GC content. V13 was most closely related to ATCC 33809, the type strain of *V. fluvialis*, with an ANI of 98.42%. Compared with ATCC 33809, V13 possessed 262 unique genes, 176 of which could not be annotated in the COG database (Table S1). Gene ontology (GO) analysis showed that the unique genes were involved in biological process, cellular component, and molecular functions, and were enriched in cellular and metabolic processes (Figure S1A). Similarly, Kyoto Encyclopedia of Genes and Genomes (KEGG) annotation revealed that VI3-specific genes were strongly associated with metabolism (Figure S1B). Transmission electron microscopy revealed that V13 was a curved rod with a capsule and polar flagella (Figure 1A). V13 exhibited a marked diffusing growth pattern in 0.3% agar (Figure 1B), indicating that V13 possessed swimming ability. V13 could grow in the presence of 0–9% NaCl (w/v), with optimal growth occurring at 0−3% NaCl (Figure 1C). pH test showed that V13 grew at pH 5 to 10, with optimal growth occurring at pH 6 to 8 (Figure 1D). Temperature test showed that V13 could grow at 5°C–37°C, and 28°C–37°C were the optimal growth temperatures (Figure 1E). These biological features probably enabled V13 to survive the extreme deep-sea conditions, including low temperature and high salinity.

The virulence and cytotoxic potential of V13

The virulence potential of V13 was examined in a fish (turbot, *Scophthalmus maximus*) infection model, which showed that V13 exhibited an LD_{50} of 5.2×10^5 CFU (colony forming unit)/g. In the infected fish, viable V13 was recovered from blood, kidney, liver, and spleen, and the amount of the recovered bacteria in each of the tissues increased with the infection time (Figure S2). To examine the virulence potential of V13 at the cellular level, THP-1 cells (in the form of PMA-differentiated macrophages) were used. V13 induced dramatic cell death after 4 h of infection, with the dying cells becoming swollen up and releasing lactate dehydrogenase (LDH) (Figures 2A–2C). LDH is a large cytosolic enzyme that is released extracellularly when the plasma membrane integrity is severely perturbed such as in the case of pyroptosis and necroptosis. As such, LDH release is commonly used as an indicator of serious plasma membrane damage or cell death. In V13-treated THP-1 cells, LDH release was time-dependent and inhibited by the pyroptosis inhibitor necrosulfonamide (NSA), but not by the necroptosis inhibitor (Nec-1s) or the apoptosis inhibitor (Z-DEVD-FMK) (Figures 2C and 2D). In addition to THP-1 cells, V13 was also cytotoxic to sheep red blood cells, HeLa cells, and GES-1 cells (Figure 2E; Figure S3A).

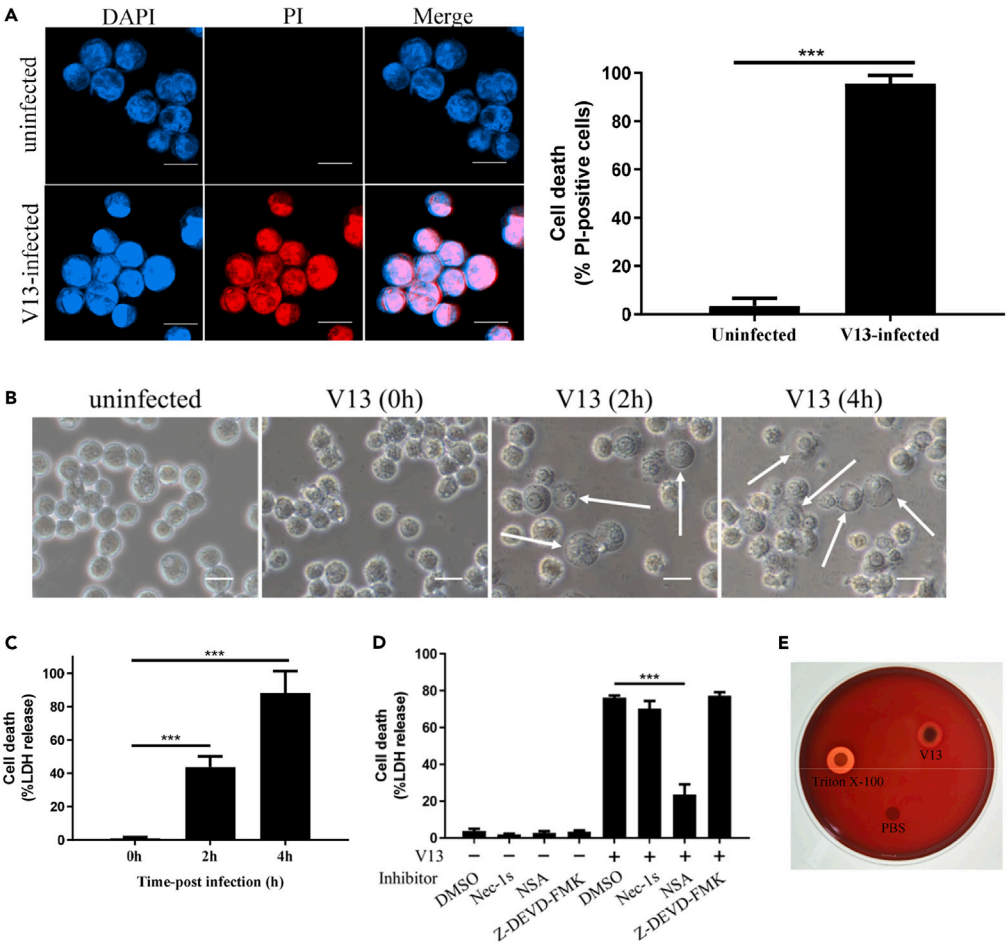

Figure 2. The virulence and cytotoxic activity of V13

(A) THP-1 cells were incubated with or without V13 for 4 h. The cells were stained with DAPI and PI, and then observed with a confocal microscope. Scale bar, 10 μm. The percentages of PI-positive cells are shown on the right panel.

(B) The morphology of the THP-1 cells at different hours after V13 infection. Arrows indicate representative cells at different stages of death. Scale bar, 10 μm.

(C) LDH release from THP-1 cells at different hours after V13 infection.

(D) THP-1 cells were pretreated with Nec-1s, necrosulfonamide (NSA), Z-DEVD-FMK, or DMSO for 1 h and then infected with or without V13 for 4 h. LDH release was then determined.

(E) V13, 2% Triton X-100, and PBS were spotted onto the filter discs in a sheep blood agar plate. Hemolysis was observed after 24 h incubation. The data in (A), (C), and (D) are the means of triplicate experiments and shown as means ± standard deviation (SD). ***$p < 0.001$.

V13 induces cell death by activation of the pyroptosis pathway

Since the morphology of V13-induced cell death resembled pyroptosis and inhibited specifically by pyroptosis inhibitor, the potential involvement of the molecules associated with the pyroptosis pathway i.e., caspase 1 (Casp1), NLRP3, apoptosis-associated speck-like protein containing a CARD (ASC), and gasdermin D (GSDMD), was examined using cells defective in either of these molecules. The results showed that when V13 infection was performed with THP-1 cells with Casp1 knockdown (Casp1-KD), NLRP3 knockdown (NLRP3-KD), ASC knockout (ASC-KO), or GSDMD knockout (GSDMD-KO), LDH release and the production of IL-1β and IL-18 were significantly reduced (Figures 3A and 3B), suggesting importance of the pyroptosis pathway in the realization of V13 cytotoxicity. Consistently, western blot showed that V13 induced-cell death required the activation of Casp1 and GSDMD, and blocking NLRP3, Casp1, or GSDMD activation by inhibitor significantly rescued the cells from V13-induced death (Figures 3C–3E).

The δVFH gene is vital to V13-induced cell death in the genetic background of VFH knockout

To examine whether V13 executed its cytotoxic effect extracellularly or intracellularly, V13 infection was carried out in the presence of the phagocytosis inhibitors cytochalasin B and D, which may block the intracellular trafficking of V13. Indeed, these inhibitors dramatically reduced the intracellular load of V13 in THP-1 cells but did not affect the ability of V13 to induce cell death (Figures 4A and 4B). This

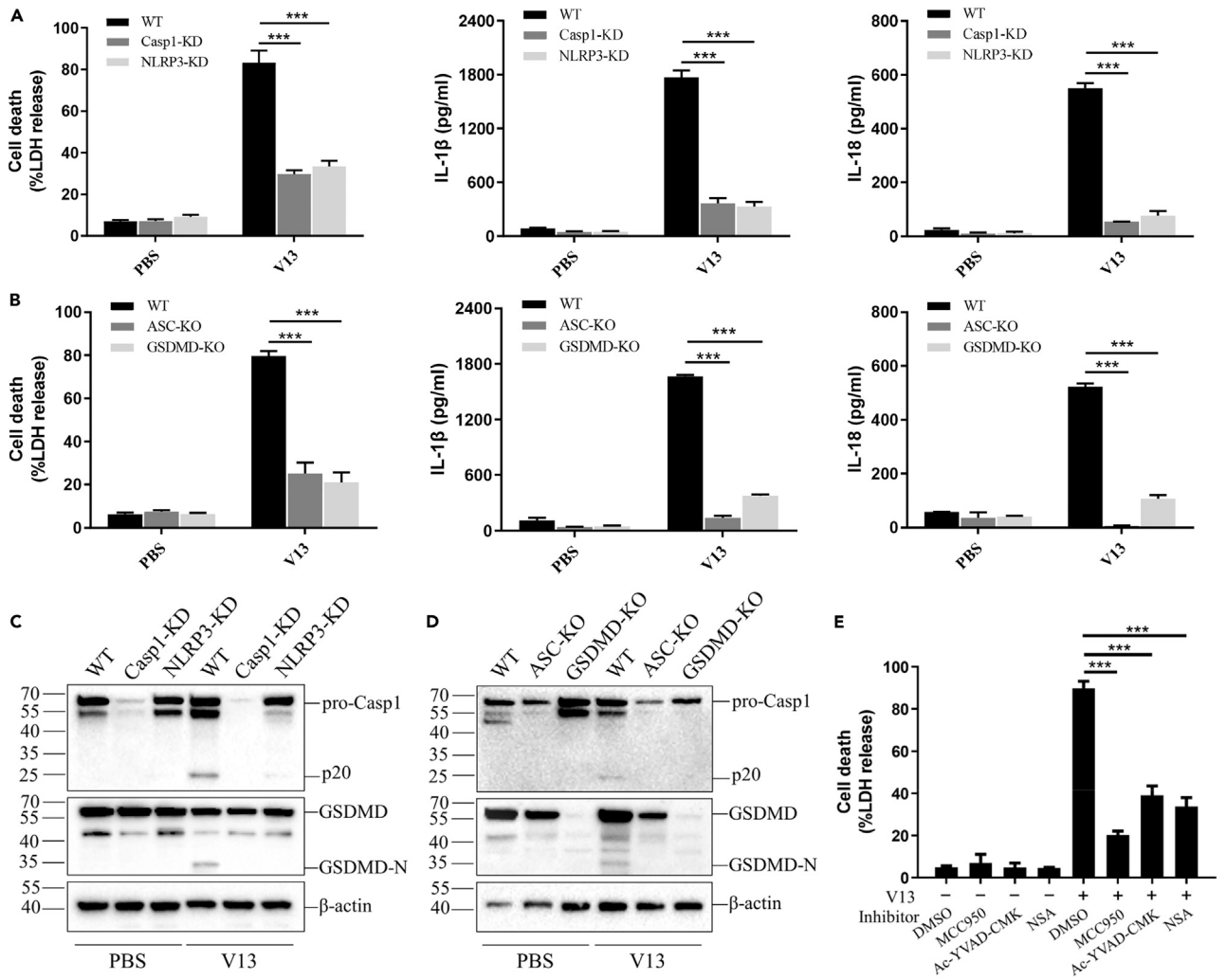

Figure 3. The involvement of the pyroptosis pathway in V13-induced cell death

(A and B) PBS or V13 was incubated with wild type (WT) THP-1 cells or THP-1 cells defective in Casp1 (Casp1-KD), NLRP3 (NLRP3-KD), ASC (ASC-KO), or GSDMD (GSDMD-KO) for 4 h. LDH, IL-1β, and IL-18 releases were then determined.

(C and D) The cells of (A) and (B) were subjected to western blot with anti-Casp1, anti-GSDMD, or anti-β-actin (loading control) antibodies.

(E) THP-1 cells were pretreated with the inhibitor MCC950, Ac-YVAD-CMK, or NSA for 1 h, and then infected with or without V13 for 4 h. LDH release was then determined. The data in (A), (B), and (E) are the means of triplicate experiments and shown as means ± standard deviation (SD). ***$p < 0.001$.

observation suggested that V13 could trigger pyroptosis effectively from outside of the cells via extracellular factors, which might be hemolysins. A survey of the V13 genome identified four hemolysin genes, two of which encoded VFH and δVFH, respectively (Table S2). To examine whether these hemolysins were involved in V13 virulence, VFH and δVFH were either deleted separately to create single gene knockouts (V13ΔVFH and V13ΔδVFH, respectively) or deleted together to create the double-gene knockout (V13ΔVFHΔδVFH). The intracellular uptakes of the mutant strains by THP-1 cells were similar to that of the wild-type V13 (Figure S4A). V13ΔVFH and V13ΔδVFH still retained hemolytic capacity, whereas V13ΔVFHΔδVFH completely lost hemolytic activity (Figure S4B). When incubated with THP-1 cells, V13ΔδVFH induced LDH release in a manner similar to V13, whereas V13ΔVFH induced a significantly lower amount of LDH release compared to V13, and V13ΔVFHΔδVFH induced LDH release in a manner that was not only significantly lower than V13 but also significantly lower than V13ΔVFH (Figure 4C). The LDH release induced by V13ΔVFHΔδVFH/δVFH (the δVFH complement strain of V13ΔVFHΔδVFH) was comparable to that induced by V13ΔVFH (Figure S4C), indicating that the significantly decreased cell-death inducing ability (comparing with V13ΔVFH) of V13ΔVFHΔδVFH was indeed caused by δVFH knockout. Western blot showed that in the cells infected with V13ΔVFHΔδVFH, both Casp1 and GSDMD cleavages were markedly impaired (Figure 4D). Since compared with V13ΔVFHΔδVFH, V13ΔVFH exhibited a significantly stronger death-inducing capacity as reflected by LDH release, we examined whether this death-inducing effect retained by V13ΔVFH, which was most likely mediated by δVFH, was also exerted via the pyroptosis pathway. The result showed that indeed, when NLRP3, Casp1, or GSDMD was inhibited during V13ΔVFH infection of THP-1 cells, LDH release was significantly decreased (Figure 4E). Given the strong cytotoxicity of

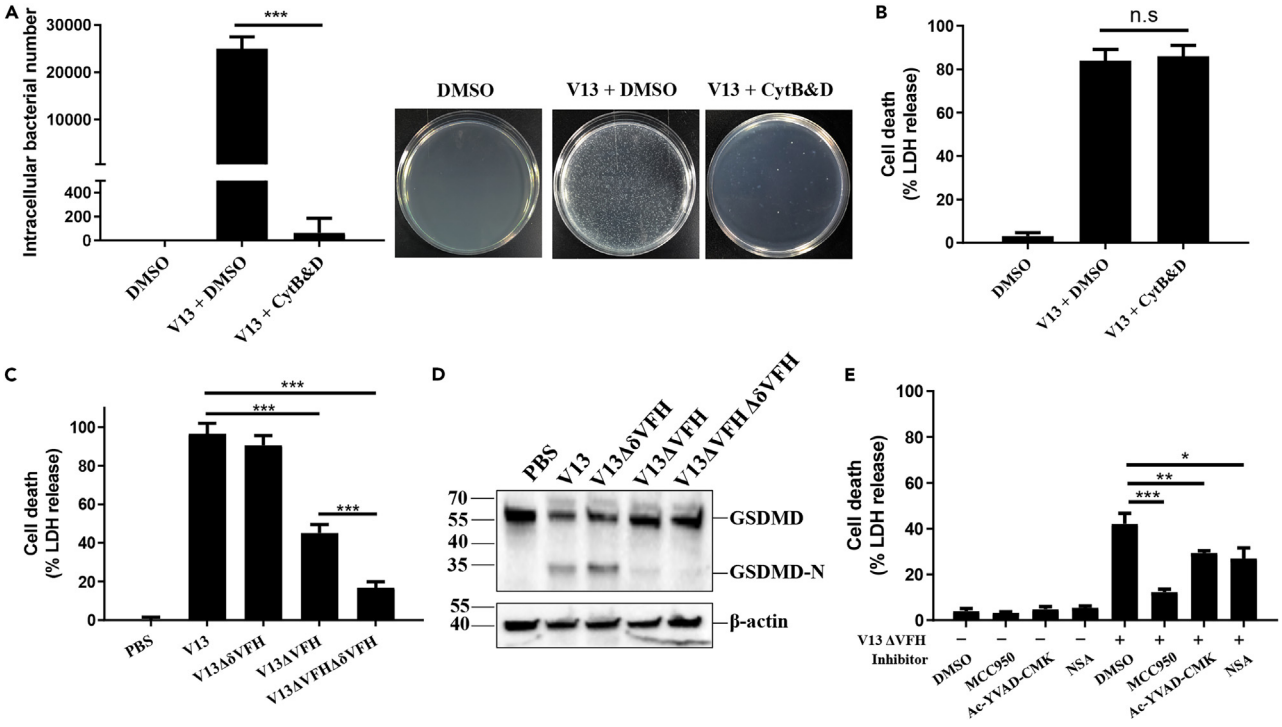

Figure 4. The role of δVFH in V13-induced pyroptosis

(A) THP-1 cells were pretreated with cytochalasin B and D (CytbB&D) or DMSO and then infected with or without V13 for 4 h. The intracellular bacterial number was determined by plate count.

(B) THP-1 cells were pretreated with CytbB&D or DMSO as aforementioned and then infected with or without V13 for 4 h. LDH release was recorded.

(C) THP-1 cells were infected with PBS, V13 or its mutants for 4 h. LDH release was then determined.

(D) The cells of (C) were subjected to western blot with anti-GSDMD or anti-β-actin (loading control) antibodies.

(E) THP-1 cells were pretreated with the inhibitor MCC950, Ac-YVAD-CMK, or NSA for 1 h, and then infected with or without V13ΔVFH for 4 h. LDH release was then determined. The data of all histograms are the means of triplicate experiments and shown as means ± standard deviation (SD). n.s, no significance, *p < 0.05, **p < 0.01, ***p < 0.001.

VFH and δVFH, we examined the prevalence of these two genes in *V. fluvialis*. For this purpose, we analyzed the genomic data of 306 *V fluvialis* isolates (149 clinical and 157 environmental) in the Pathogen Detection of NCBI database (https://www.ncbi.nlm.nih.gov/pathogens/) (Table S3). The results showed that 305 strains possessed VFH and δVFH homologous sequences, which share over 96% identity with V13 VFH and δVFH (Table S3).

δVFH triggers NLRP3 inflammasome-mediated, K^+- and Ca^{2+}-regulated pyroptosis

Western blot showed that δVFH was detected in the culture supernatant of V13ΔδVFH/δVFH, in which δVFH was expressed as a His-tagged protein (Figure S5), indicating that δVFH was a secreted protein. To examine the potential cytotoxic effect of δVFH as a free toxin, recombinant protein of δVFH was purified. When incubated with THP-1 cells, δVFH induced pyroptosis-like cell death in a dose-dependent manner, accompanied with LDH release and the activation cleavage of Casp1 and GSDMD (Figures 5A–5C). THP-1 cells incubated with the control protein small ubiquitin-like modifier (SUMO) exhibited no apparent cell death (data not shown). δVFH was also cytotoxic to sheep red blood cells, HeLa cells, and GES-1 cells (Figures S3B and S4B). When δVFH was incubated with the THP-1 cells defective in Casp1 (Casp1-KD), NLRP3 (NLRP3-KD), ASC (ASC-KO), or GSDMD (GSDMD-KO), LDH release, and Casp1/GSDMD activation were significantly reduced (Figures 5D and 5E). Similarly, when δVFH was incubated with THP-1 cells in the presence of the inhibitor against NLRP3 (MCC950), Casp1 (Ac-YVAD-CMK), or GSDMD (NSA), cell death was significantly inhibited in a manner that depended on the dose of the inhibitor (Figures 5F–5H). These results indicated that δVFH induced NLRP3-mediated pyroptosis. Furthermore, supplementation of extracellular K^+, or blocking intracellular Ca^{2+} by the chelator BAPTA-AM, inhibited δVFH-induced Casp1 and GSDMD cleavage in a manner that depended on the dose of the supplemented K^+ and the Ca^{2+} chelator (Figures 5I and 5J).

δVFH binds host cells and interacts with specific cellular lipids

Microscopy showed that following incubation with THP-1 cells, δVFH was localized at the cellular membrane (Figure 6A). Since some cytotoxins are known to target the plasma membrane via interaction with membrane lipids, we examined the potential interaction between

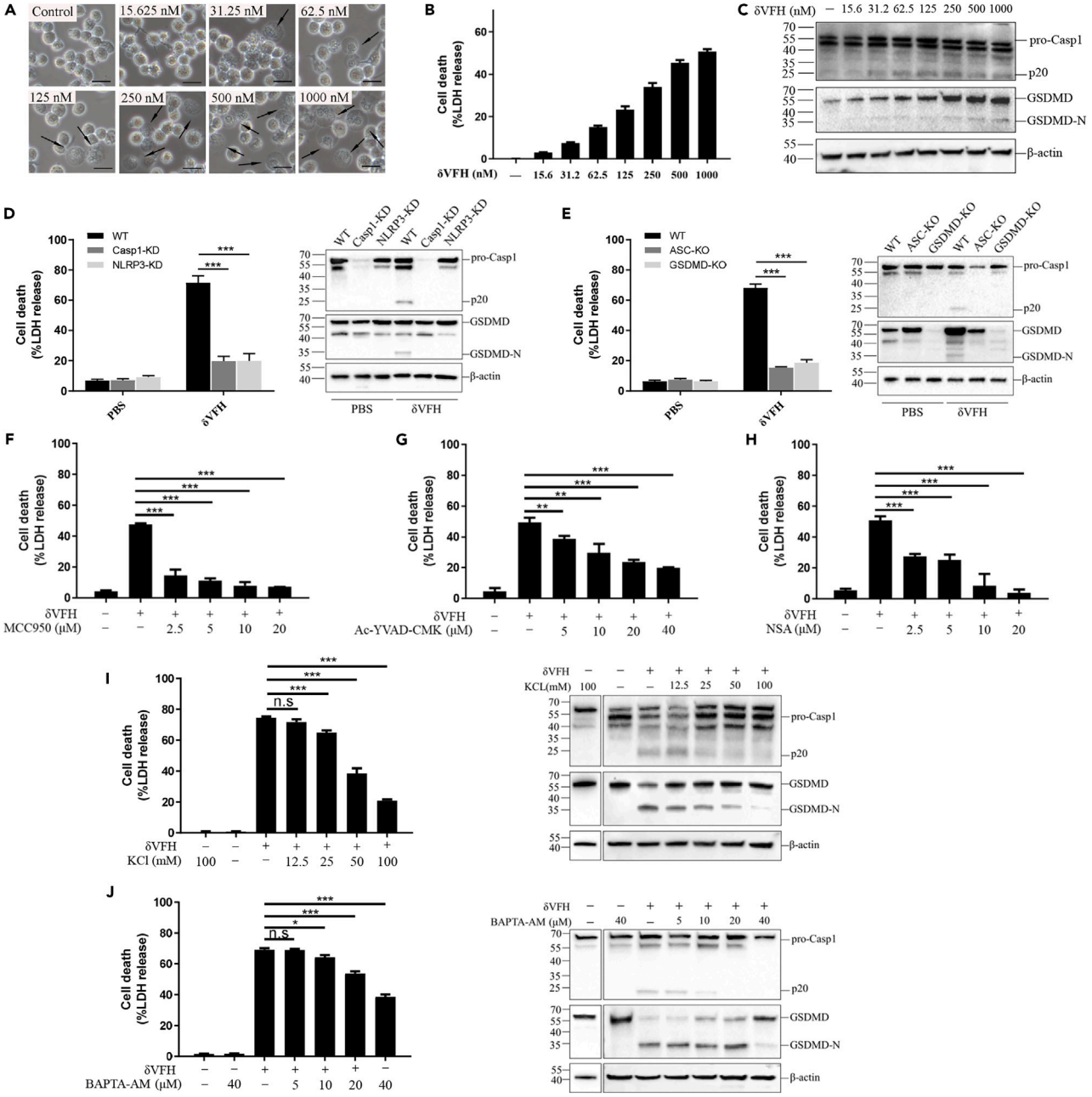

Figure 5. The cytotoxicity of δVFH

(A–C) THP-1 cells were incubated with or without (Control) different concentrations of δVFH for 2 h and then subjected to microscopic observation (A), LDH release determination (B), and western blot using anti-Casp1, anti-GSDMD, or anti-β-actin (loading control) antibodies (C). The arrows in (A) indicate representative cells at different stages of death. Scale bar, 10 μm.

(D) PBS or δVFH was incubated with wild type (WT) THP-1 cells or THP-1 cells defective in Casp1 (Casp1-KD) or NLRP3 (NLRP3-KD) for 2 h. The cells were subjected to LDH release determination (left) and western blot using anti-Casp1, anti-GSDMD, or anti-β-actin (loading control) antibodies (right).

(E) PBS or δVFH was incubated with wild type (WT) THP-1 cells or THP-1 cells defective in ASC (ASC-KO) or GSDMD (GSDMD-KO) for 2 h. The cells were subjected to LDH release determination (left) and western blot (right) as aforementioned.

(F–H) THP-1 cells were pretreated with different concentrations of the inhibitor MCC950 (F), Ac-YVAD-CMK (G), or NSA (H) for 1 h, and then treated with δVFH for 2 h. LDH release was then determined.

(I and J) THP-1 cells were treated with or without KCl (0–100 mM) (I) or BAPTA-AM (0–40 μM) (J) for 45 min and then incubated with δVFH for 2 h. The cells were subjected to LDH release determination (left panels) and western blot using anti-Casp1, anti-GSDMD, or anti-β-actin (loading control) antibodies (right panels). The results of all histograms are the means of triplicate experiments and shown as means ± standard deviation (SD). *$p < 0.05$, **$p < 0.01$, ***$p < 0.001$.

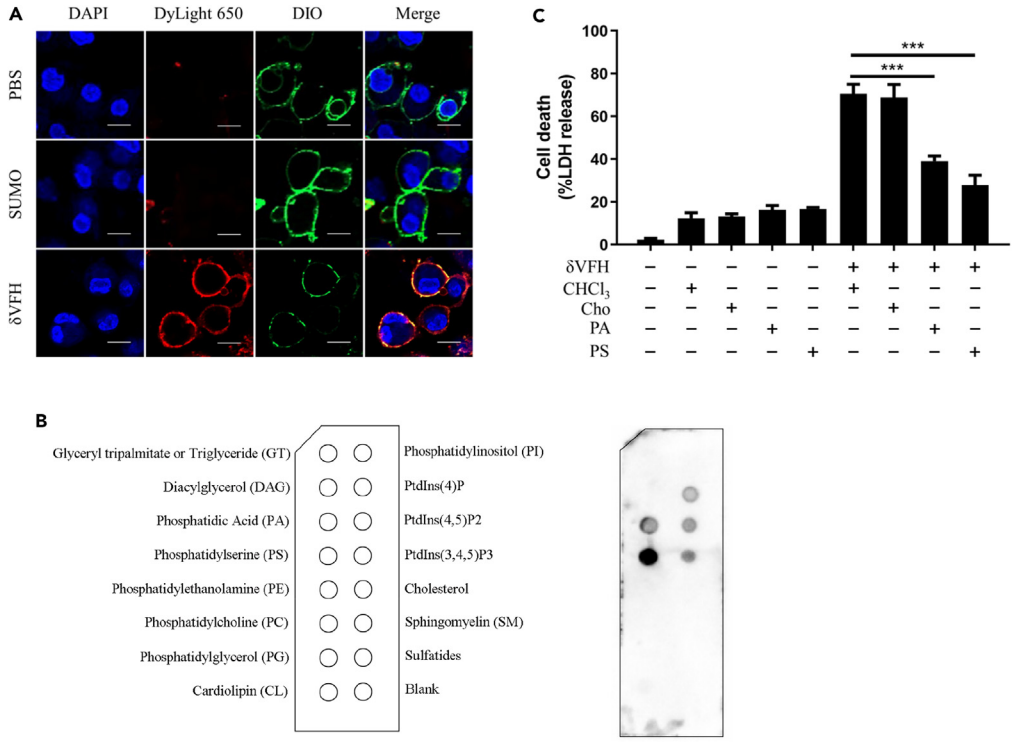

Figure 6. Interaction of δVFH with cellular membrane and lipids

(A) THP-1 cells were incubated with PBS, δVFH, or SUMO (control protein) for 1 h. The cells were then treated with DyLight650 anti-His antibody and observed with a confocal microscope. Scale bar, 10 μm.

(B) A membrane lipid strip containing 15 different lipids (left) was incubated with δVFH for 1 h and then probed with anti-His antibody (right).

(C) THP-1 cells were incubated with or without δVFH that had been pre-treated with cholesterol (Cho), phosphatidylserine (PS), phosphatidic acid (PA), or $CHCl_3$ (control). After 2 h incubation, LDH release was determined. Data are the means of triplicate experiments and shown as means ± standard deviation (SD). ***$p < 0.001$.

δVFH and 15 lipids on a lipid strip. The result showed that δVFH exhibited apparent binding to phosphatidylserine (PS) and, to less extents, phosphatidic acid (PA), PtdIns(4)P, PtdIns(4,5)P2, and PtdIns(3,4,5)P3 (Figure 6B). When δVFH was pretreated with PS or PA, its ability to induce LDH release from THP-1 cells was significantly reduced (Figure 6C). In contrast, pretreatment with cholesterol, to which δVFH did not bind (Figure 6B), had no significant effect on the cytotoxicity of δVFH (Figure 6C).

DISCUSSION

In this study, we examined the virulence property of a deep-sea *V. fluvialis* isolate, V13. V13 was most closely related to the *V. fluvialis* type strain ATCC 33809. However, V13 was able to grow not only in high salt conditions but also in the absence of NaCl, a phenotype also observed in *Vibrio viridaestus* and *Vibrio hippocampi* from marine environments.[29,30] These results suggest a strong environmental adaptation ability of marine Vibrios. Although V13 shares a high ANI with *V. fluvialis* ATCC 33809, it still possesses 262 unique genes. Since most of the unique genes are hypothetical and have no known counterparts in the available databank, they may function in the adaptation of V13 to the deep-sea environment. Both GO and KEGG analyses showed that the unique genes of V13 were mainly involved in metabolic and cellular processes, suggesting a role of these genes in the specific metabolisms and cellular activities required for deep-sea survival. In contrast, the gene encoding trimethylamine-N-oxide reductase TorA, which was reported to enhance the pressure tolerance of *V. fluvialis*,[28] is present in both V13 and *V. fluvialis* ATCC 33809, suggesting that TorA may be functionally essential in both high-pressure environments and normal pressure environments.

Recently, several gram-positive bacteria, in particular bacillus, from deep sea have been reported to be pathogenic to vertebrate animals.[31–33] For deep-sea vibrios, a *Vibrio antiquaries* strain from the hydrothermal vent in the East Pacific Rise was reported to encode virulence factors known to be involved in human disease.[25] However, it is not clear whether this *V. antiquaries* isolate is capable of infection. In our study, *in vivo* infection showed that V13 was able to disseminate in fish tissues and cause mortality. Cellular study showed that like the human *V. fluvialis* isolate, which exerted cytotoxic effects on human and Chinese hamster cells,[9,10] V13 was cytotoxic to THP-1 cells by activation of the pyroptosis pathway involving Casp1, GSDMD, and NLRP3. Together, these results indicated a pathogenic and cytotoxic nature of V13.

For all the pathogenic genera of *Vibrio*, most of the virulence effectors are secreted toxins with perforation capacity.[15] For *V. fluvialis*, VFH was demonstrated to be a virulence factor that could induce the secretion of IL-1β mediated by the NLRP3 inflammasome in mouse macrophages.[18] Currently, the roles of the hemolysins other than VFH, such as δVFH, in *V. fluvialis* pathogenicity are unknown. In this study, we found that compared with the wild type V13, the VFH mutant (V13ΔVFH) was significantly reduced in cytotoxicity, whereas the δVFH mutant (V13ΔδVFH) was barely affected in cytotoxicity. We speculated that the toxicity of VFH may be so strong as to mask the effect of δVFH as well as other virulence factors. To examine whether this was the case, the VFH-δVFH double mutant, V13ΔVFHΔδVFH, was constructed and examined. Indeed, the cytotoxicity of V13ΔVFHΔδVFH was significantly lower not only than that of V13 but also than that of V13ΔVFH, implying that δVFH played a significant role in the pathogenicity of V13. Unlike *V. parahaemolyticus* TDH and *V. cholerae* cholera toxin (CT), which are rarely detected from environmental isolates[34–36] and probably function specifically in infection, we found that δVFH, as well as VFH, homologs are widely distributed in both clinical and environmental *V. fluvialis* isolates, suggesting that these hemolysins may be beneficial for bacterial survival under both clinical and non-clinical conditions. Previous studies showed that in *V. parahaemolyticus*, δVPH (homologous to δVFH) as well as other thermostable hemolysins (TDH, TRH, and TLH (thermolabile hemolysin)) were indispensable virulence factors, which entered host cells via the type III secretion system of the bacteria and activated autophagy effectors, ultimately causing cell death.[21,37] In our study, we found that δVFH was secreted extracellularly by V13ΔδVFH/δVFH, and the gene clusters associated with three secretion systems—the type II, III, and VI secretion systems—existed in the genome of V13. Whether these secretion systems are involved in δVFH secretion remains to be examined in future studies.

Pyroptosis is a type of programmed cell death induced by various stimuli, including bacterial infection. Many bacterial pathogens, such as *Mycobacterium tuberculosis* and *Yersinia pestis*, activate pyroptosis through different pathways.[38–41] Some bacterial toxins, such as the pore-forming leucocidin of *Vibrio proteolyticus*, the VFH of *V. fluvialis*, and the cytotoxins (Nhe, Hbl, and CytK) of *B. cereus*,[18,42–45] can directly provoke pyroptosis.[45] Similarly, in the case of δVFH, we found that it alone induced robust pyroptosis by promoting NLRP3-mediated Casp1 cleavage and GSDMD activation in a manner similar to V13, suggesting that δVFH probably contributed at least in part to the pyroptotic cell death triggered by V13. Previous studies have shown that the assembly of the NLPR3 inflammasome complex is induced by multiple factors, including the efflux of K^+ and the accumulation of intracellular Ca^{2+}.[46–48] In the present study, we found that either prevention of intracellular K^+ loss by supplementation of extracellular K^+ or blocking Ca^{2+} accumulation by chemical chelation significantly inhibited δVFH-induced pyroptosis. These results indicated that the NLPR3 signaling pathway induced by δVFH was regulated by K^+ and Ca^{2+}. Hence, inhibition of NLRP3 inflammasome activation might be a strategy for the development of antimicrobials against V13.

As pore-forming toxins, thermostable hemolysins may interact with cellular membrane by binding to membrane lipids.[49] For δVFH, we found that it bound strongly to PS, as well as PA and various phosphoinositides. Consistently, pretreatment of δVFH with PS or PA significantly impaired the ability of δVFH to induce cell death, indicating a vital role of membrane lipid interaction in the cytotoxicity of δVFH. Phosphorylserine is involved in the activation of the FAK-SRC-STAT3 signaling pathway[50]; PA and phosphoinositides are regulators of many cellular signaling processes and membrane structure.[51,52] Given the importance of these phospholipids in plasma membrane composition and cell signaling, it is possible that the binding of δVFH to these lipids may cause membrane rearrangement or alter cellular activity in a way that leads to pyroptosis.

In conclusion, in this study we demonstrated that pathogenic *V. fluvialis* existed in deep sea. We showed that the pathogenic *V. fluvialis* possessed both unique genes and common virulence genes ubiquitously present in human clinical isolates. The bacterial toxins of VFH and δVFH played a crucial role in the cytotoxicity of *V. fluvialis*. δVFH exerted its cytotoxic effect by binding to plasma membrane lipids and induced NLRP3-mediated pyroptosis. These findings promoted our understanding of the ecological distribution and virulence mechanism of *V. fluvialis*.

Limitations of the study

Although this study discovered the membrane lipids bound by δVFH and required for δVFH cytotoxicity, the detailed interaction mechanism between these lipids and δVFH is unclear. In addition, the potential roles of the unique genes in V13 adaptation to the deep-sea environment remain to be investigated.

STAR★METHODS

Detailed methods are provided in the online version of this paper and include the following:

- KEY RESOURCES TABLE
- RESOURCE AVAILABILITY
  - Lead contact
  - Materials availability
  - Data and code availability
- EXPERIMENTAL MODEL AND STUDY PARTICIPANT DETAIL
  - Animals
  - Cells and bacteria
- METHOD DETAILS
  - Bacterial culture and observation

- Cell culture
- Genome sequencing and unique gene analysis
- *In vivo* bacterial infection
- Construction of V13 mutants and complementary strains
- Purification of recombinant δVFH
- The cytotoxic effects of V13 variants and δVFH
- Hemolysis assay
- Cytokine production analysis
- Immunoblot
- δVFH binding to cells and lipids

SUPPLEMENTAL INFORMATION

Supplemental information can be found online at https://doi.org/10.1016/j.isci.2024.109558.

ACKNOWLEDGMENTS

This work was supported by the Strategic Priority Research Program of the Chinese Academy of Sciences (XDA22050402 and XDA22050403), the Innovation Research Group Project of the National Natural Science Foundation of China (42221005), and Shandong Postdoctoral Science Foundation (SDCX-ZG-202303040).

AUTHOR CONTRIBUTIONS

L.S., Y.Z., and J.L. designed the study. J.Z. isolated and analyzed the bacteria. Y.W., J.L., and Y.Z. conducted the experiments. Y.W., J.L., Y.Z., and X.G. analyzed the data. J.L. wrote the first draft of the manuscript. L.S. edited the manuscript.

DECLARATION OF INTERESTS

The authors declare no competing interests.

Received: August 13, 2023
Revised: December 19, 2023
Accepted: March 22, 2024
Published: March 26, 2024

REFERENCES

1. Baker-Austin, C., Trinanes, J., Gonzalez-Escalona, N., and Martinez-Urtaza, J. (2017). Non-Cholera Vibrios: The Microbial Barometer of Climate Change. Trends Microbiol. *25*, 76–84.
2. Trinanes, J., and Martinez-Urtaza, J. (2021). Future scenarios of risk of Vibrio infections in a warming planet: a global mapping study. Lancet Planet. Health *5*, e426–e435.
3. Oliver, J.D. (2005). Wound infections caused by Vibrio vulnificus and other marine bacteria. Epidemiol. Infect. *133*, 383–391.
4. Karaolis, D.K., Johnson, J.A., Bailey, C.C., Boedeker, E.C., Kaper, J.B., and Reeves, P.R. (1998). A Vibrio cholerae pathogenicity island associated with epidemic and pandemic strains. Proc. Natl. Acad. Sci. USA *95*, 3134–3139.
5. Ali, M., Lopez, A.L., You, Y.A., Kim, Y.E., Sah, B., Maskery, B., and Clemens, J. (2012). The global burden of cholera. Bull. World Health Organ. *90*, 209–218a.
6. Altekruse, S.F., Bishop, R.D., Baldy, L.M., Thompson, S.G., Wilson, S.A., Ray, B.J., and Griffin, P.M. (2000). Vibrio gastroenteritis in the US Gulf of Mexico region: the role of raw oysters. Epidemiol. Infect. *124*, 489–495.
7. Yun, N.R., and Kim, D.M. (2018). Vibrio vulnificus infection: a persistent threat to public health. Korean J. Intern. Med. (Engl. Ed.) *33*, 1070–1078.
8. Ramamurthy, T., Chowdhury, G., Pazhani, G.P., and Shinoda, S. (2014). Vibrio fluvialis: an emerging human pathogen. Front. Microbiol. *5*, 91.
9. Fink, S.L., and Cookson, B.T. (2005). Apoptosis, pyroptosis, and necrosis: mechanistic description of dead and dying eukaryotic cells. Infect. Immun. *73*, 1907–1916.
10. Kothary, M.H., Lowman, H., McCardell, B.A., and Tall, B.D. (2003). Purification and characterization of enterotoxigenic El Tor-like hemolysin produced by Vibrio fluvialis. Infect. Immun. *71*, 3213–3220.
11. Li, L., Meng, H., Gu, D., Li, Y., and Jia, M. (2019). Molecular mechanisms of Vibrio parahaemolyticus pathogenesis. Microbiol. Res. *222*, 43–51.
12. Vanden Broeck, D., Horvath, C., and De Wolf, M.J.S. (2007). Vibrio cholerae: cholera toxin. Int. J. Biochem. Cell Biol. *39*, 1771–1775.
13. Yoon, S.H., and Waters, C.M. (2019). Vibrio cholerae. Trends Microbiol. *27*, 806–807.
14. Gxalo, O., Digban, T.O., Igere, B.E., Olapade, O.A., Okoh, A.I., and Nwodo, U.U. (2021). Virulence and Antibiotic Resistance Characteristics of Vibrio Isolates From Rustic Environmental Freshwaters. Front. Cell. Infect. Microbiol. *11*, 732001.
15. Mohamad, N., Amal, M.N.A., Saad, M.Z., Yasin, I.S.M., Zulkiply, N.A., Mustafa, M., and Nasruddin, N.S. (2019). Virulence-associated genes and antibiotic resistance patterns of Vibrio spp. isolated from cultured marine fishes in Malaysia. BMC Vet. Res. *15*, 176.
16. Vesth, T., Wassenaar, T.M., Hallin, P.F., Snipen, L., Lagesen, K., and Ussery, D.W. (2010). On the origins of a Vibrio species. Microb. Ecol. *59*, 1–13.
17. Wall, V.W., Kreger, A.S., and Richardson, S.H. (1984). Production and partial characterization of a Vibrio fluvialis cytotoxin. Infect. Immun. *46*, 773–777.
18. Song, L., Huang, Y., Zhao, M., Wang, Z., Wang, S., Sun, H., Kan, B., Meng, G., Liang, W., and Ren, Z. (2015). A critical role for hemolysin in Vibrio fluvialis-induced IL-1β secretion mediated by the NLRP3 inflammasome in macrophages. Front. Microbiol. *6*, 510.
19. Cai, Q., and Zhang, Y. (2018). Structure, function and regulation of the thermostable direct hemolysin (TDH) in pandemic Vibrio parahaemolyticus. Microb. Pathog. *123*, 242–245.
20. Raghunath, P. (2014). Roles of thermostable direct hemolysin (TDH) and TDH-related hemolysin (TRH) in Vibrio parahaemolyticus. Front. Microbiol. *5*, 805.
21. Zhang, L., and Orth, K. (2013). Virulence determinants for Vibrio parahaemolyticus infection. Curr. Opin. Microbiol. *16*, 70–77.

22. Brazelton, W. (2017). Hydrothermal vents. Curr. Biol. *27*, R450–r452.
23. Wang, W., Li, Z., Zeng, L., Dong, C., and Shao, Z. (2020). The oxidation of hydrocarbons by diverse heterotrophic and mixotrophic bacteria that inhabit deep-sea hydrothermal ecosystems. ISME J. *14*, 1994–2006.
24. Delbarre-Ladrat, C., Salas, M.L., Sinquin, C., Zykwinska, A., and Colliec-Jouault, S. (2017). Bioprospecting for Exopolysaccharides from Deep-Sea Hydrothermal Vent Bacteria: Relationship between Bacterial Diversity and Chemical Diversity. Microorganisms *5*, 63.
25. Hasan, N.A., Grim, C.J., Lipp, E.K., Rivera, I.N.G., Chun, J., Haley, B.J., Taviani, E., Choi, S.Y., Hoq, M., Munk, A.C., et al. (2015). Deep-sea hydrothermal vent bacteria related to human pathogenic Vibrio species. Proc. Natl. Acad. Sci. USA *112*, E2813–E2819.
26. Lasa, A., Auguste, M., Lema, A., Oliveri, C., Borello, A., Taviani, E., Bonello, G., Doni, L., Millard, A.D., Bruto, M., et al. (2021). A deep-sea bacterium related to coastal marine pathogens. Environ. Microbiol. *23*, 5349–5363.
27. Martins, A., Tenreiro, T., Andrade, G., Gadanho, M., Chaves, S., Abrantes, M., Calado, P., Tenreiro, R., and Vieira, H. (2013). Photoprotective bioactivity present in a unique marine bacteria collection from Portuguese deep sea hydrothermal vents. Mar. Drugs *11*, 1506–1523.
28. Yin, Q.J., Zhang, W.J., Qi, X.Q., Zhang, S.D., Jiang, T., Li, X.G., Chen, Y., Santini, C.L., Zhou, H., Chou, I.M., and Wu, L.F. (2017). High Hydrostatic Pressure Inducible Trimethylamine N-Oxide Reductase Improves the Pressure Tolerance of Piezosensitive Bacteria Vibrio fluvialis. Front. Microbiol. *8*, 2646.
29. Li, Y., Liang, J., Liu, R., Xue, C.X., Zhou, S., He, X., Li, B., Wang, X., and Zhang, X.H. (2020). Vibrio sinensis sp. nov. and Vibrio viridaestus sp. nov., two marine bacteria isolated from the East China Sea. Int. J. Syst. Evol. Microbiol. *70* (2), 889–896.
30. Balcázar, J.L., Pintado, J., and Planas, M. (2010). Vibrio hippocampi sp. nov., a new species isolated from wild seahorses (Hippocampus guttulatus). FEMS Microbiol. Lett. *307* (1), 30–34.
31. Sun, Y.Y., Chi, H., and Sun, L. (2016). Pseudomonas fluorescens Filamentous Hemagglutinin, an Iron-Regulated Protein, Is an Important Virulence Factor that Modulates Bacterial Pathogenicity. Front. Microbiol. *7*, 1320.
32. Gu, H.J., Sun, Q.L., Luo, J.C., Zhang, J., and Sun, L. (2019). A First Study of the Virulence Potential of a Bacillus subtilis Isolate From Deep-Sea Hydrothermal Vent. Front. Cell. Infect. Microbiol. *9*, 183.
33. Wang, Y., Zhang, J., Yuan, Z., and Sun, L. (2022). Characterization of the pathogenicity of a Bacillus cereus isolate from the Mariana Trench. Virulence *13*, 1062–1075.
34. Ceccarelli, D., Hasan, N.A., Huq, A., and Colwell, R.R. (2013). Distribution and dynamics of epidemic and pandemic Vibrio parahaemolyticus virulence factors. Front. Cell. Infect. Microbiol. *3*, 97.
35. Kurazono, H., Pal, A., Bag, P.K., Nair, G.B., Karasawa, T., Mihara, T., and Takeda, Y. (1995). Distribution of genes encoding cholera toxin, zonula occludens toxin, accessory cholera toxin, and El Tor hemolysin in Vibrio cholerae of diverse origins. Microb. Pathog. *18*, 231–235.
36. Faruque, S.M., Chowdhury, N., Kamruzzaman, M., Dziejman, M., Rahman, M.H., Sack, D.A., Nair, G.B., and Mekalanos, J.J. (2004). Genetic diversity and virulence potential of environmental Vibrio cholerae population in a cholera-endemic area. Proc. Natl. Acad. Sci. USA *101*, 2123–2128.
37. Cornelis, G.R. (2006). The type III secretion injectisome. Nat. Rev. Microbiol. *4*, 811–825.
38. Beckwith, K.S., Beckwith, M.S., Ullmann, S., Sætra, R.S., Kim, H., Marstad, A., Åsberg, S.E., Strand, T.A., Haug, M., Niederweis, M., et al. (2020). Plasma membrane damage causes NLRP3 activation and pyroptosis during Mycobacterium tuberculosis infection. Nat. Commun. *11*, 2270.
39. Sharma, B.R., Karki, R., and Kanneganti, T.D. (2019). Role of AIM2 inflammasome in inflammatory diseases, cancer and infection. Eur. J. Immunol. *49*, 1998–2011.
40. Xia, S., Hollingsworth, L.R., 4th, and Wu, H. (2020). Mechanism and Regulation of Gasdermin-Mediated Cell Death. Cold Spring Harbor Perspect. Biol. *12*, a036400.
41. Zhou, C.B., and Fang, J.Y. (2019). The role of pyroptosis in gastrointestinal cancer and immune responses to intestinal microbial infection. Biochim. Biophys. Acta Rev. Cancer *1872*, 1–10.
42. Zhao, Y., and Sun, L. (2022). Bacillus cereus cytotoxin K triggers gasdermin D-dependent pyroptosis. Cell Death Dis. *8*, 305.
43. Cohen, H., Baram, N., Edry-Botzer, L., Munitz, A., Salomon, D., and Gerlic, M. (2020). Vibrio pore-forming leukocidin activates pyroptotic cell death via the NLRP3 inflammasome. Emerg. Microb. Infect. *9*, 278–290.
44. Fox, D., Mathur, A., Xue, Y., Liu, Y., Tan, W.H., Feng, S., Pandey, A., Ngo, C., Hayward, J.A., Atmosukarto, I.I., et al. (2020). Bacillus cereus non-haemolytic enterotoxin activates the NLRP3 inflammasome. Nat. Commun. *11*, 760.
45. Mathur, A., Feng, S., Hayward, J.A., Ngo, C., Fox, D., Atmosukarto, I.I., Price, J.D., Schauer, K., Märtlbauer, E., Robertson, A.A.B., et al. (2019). A multicomponent toxin from Bacillus cereus incites inflammation and shapes host outcome via the NLRP3 inflammasome. Nat. Microbiol. *4*, 362–374.
46. Muñoz-Planillo, R., Kuffa, P., Martínez-Colón, G., Smith, B.L., Rajendiran, T.M., and Núñez, G. (2013). K^+ efflux is the common trigger of NLRP3 inflammasome activation by bacterial toxins and particulate matter. Immunity *38*, 1142–1153.
47. Paik, S., Kim, J.K., Silwal, P., Sasakawa, C., and Jo, E.K. (2021). An update on the regulatory mechanisms of NLRP3 inflammasome activation. Cell. Mol. Immunol. *18*, 1141–1160.
48. Swanson, K.V., Deng, M., and Ting, J.P.Y. (2019). The NLRP3 inflammasome: molecular activation and regulation to therapeutics. Nat. Rev. Immunol. *19*, 477–489.
49. Verma, P., and Chattopadhyay, K. (2021). Current Perspective on the Membrane-Damaging Action of Thermostable Direct Hemolysin, an Atypical Bacterial Pore-forming Toxin. Front. Mol. Biosci. *8*, 717147.
50. Liang, X., Luo, M., Shao, B., Yang, J.Y., Tong, A., Wang, R.B., Liu, Y.T., Jun, R., Liu, T., Yi, T., et al. (2022). Phosphatidylserine released from apoptotic cells in tumor induces M2-like macrophage polarization through the PSR-STAT3-JMJD3 axis. Cancer Commun. *42*, 205–222.
51. D'Angelo, G., Vicinanza, M., Di Campli, A., and De Matteis, M.A. (2008). The multiple roles of PtdIns(4)P – not just the precursor of PtdIns(4,5)P2. J. Cell Sci. *121* (Pt 12), 1955–1963.
52. Zhukovsky, M.A., Filograna, A., Luini, A., Corda, D., and Valente, C. (2019). Phosphatidic acid in membrane rearrangements. FEBS Lett. *593*, 2428–2451.
53. Sun, Q.L., Yu, C., Luan, Z.D., Lian, C., Hu, Y.H., and Sun, L. (2018). Description of Bacillus kexueae sp. nov. and Bacillus manusensis sp. nov., isolated from hydrothermal sediments. Int. J. Syst. Evol. Microbiol. *68*, 829–834.
54. Zhao, Y., Jiang, S., Zhang, J., Guan, X.L., Sun, B.G., and Sun, L. (2021). A virulent Bacillus cereus strain from deep-sea cold seep induces pyroptosis in a manner that involves NLRP3 inflammasome, JNK pathway, and lysosomal rupture. Virulence *12*, 1362–1376.
55. Li, L., Stoeckert, C.J., and Roos, D.S. (2003). OrthoMCL: identification of ortholog groups for eukaryotic genomes. Genome Res. *13*, 2178–2189.
56. Buchfink, B., Xie, C., and Huson, D.H. (2015). Fast and sensitive protein alignment using DIAMOND. Nat. Methods *12*, 59–60.
57. Zhao, Y., Chen, C., Gu, H.J., Zhang, J., and Sun, L. (2019). Characterization of the Genome Feature and Toxic Capacity of a Bacillus wiedmannii Isolate From the Hydrothermal Field in Okinawa Trough. Front. Cell. Infect. Microbiol. *9*, 370.
58. Li, M., Wu, M., Sun, Y., and Sun, L. (2022). Edwardsiella tarda TraT is an anti-complement factor and a cellular infection promoter. Commun. Biol. *5*, 637.
59. Zhang, W.w., Sun, K., Cheng, S., and Sun, L. (2008). Characterization of DegQVh, a serine protease and a protective immunogen from a pathogenic Vibrio harveyi strain. Appl. Environ. Microbiol. *74*, 6254–6262.
60. Ma, P., Li, J., Qi, L., and Dong, X. (2021). The Archaeal Small Heat Shock Protein Hsp17.6 Protects Proteins from Oxidative Inactivation. Int. J. Mol. Sci. *22* (5), 2591.
61. Qin, K., Jiang, S., Xu, H., Yuan, Z., and Sun, L. (2023). Pyroptotic gasdermin exists in Mollusca and is vital to eliminating bacterial infection. Cell Rep. *42*, 112414.
62. Li, H., Sun, Y., and Sun, L. (2022). A Teleost CXCL10 Is Both an Immunoregulator and an Antimicrobial. Front. Immunol. *13*, 917697.

STAR★METHODS

KEY RESOURCES TABLE

REAGENT or RESOURCE	SOURCE	IDENTIFIER
Antibodies		
anti-caspase 1	Cell Signaling Technology	Cat# 3866; RRID: AB_2069051
anti-GSDMD	Cell Signaling Technology	Cat# 69469
anti-actin	Abcam	Cat# ab8226; RRID: AB_306371
Goat anti-rabbit IgG H&L (HRP)	Abcam	Cat# ab97051; RRID: AB_10679369
DyLights®650 Anti-6×His antibody	Abcam	Cat# ab117504; RRID: AB_11001222
anti-DnaK	cusabio	Cat# PA633459HA01EGW
anti-ASC	ABclonal	Cat# A11433; RRID: AB_2758557
anti His-tag	ABclonal	Cat# AE086; RRID: AB_3065205
Goat anti- mouse IgG H&L (HRP)	ABclonal	Cat# AS003; RRID: AB_2769851
Goat Anti-Rabbit IgG H&L (HRP)	ABclonal	Cat# AS014; RRID: AB_2769854
Bacterial and virus strains		
Vibrio fluvialis V13	This paper	N/A
V13ΔVFH	This paper	N/A
V13ΔδVFH	This paper	N/A
V13ΔVFHΔδVFH	This paper	N/A
V13ΔVFH/VFH	This paper	N/A
V13ΔδVFH/δVFH	This paper	N/A
V13ΔVFHΔδVFH/δVFH	This paper	N/A
Escherichia coli BL21	TransGen	Cat# CD601
Biological samples		
Healthy turbot (*Scophthalmus maximus*)	A local fish farm	N/A
Chemicals, peptides, and recombinant proteins		
VFH recombinant proteins	This paper	N/A
δVFH recombinant proteins	This paper	N/A
SUMO recombinant proteins	Li et al.[62]	N/A
RPMI1640 medium	Gibco	Cat# C22400500BT
Fetal bovine serum	Gibco	Cat# 10099141C
Penicillin-Streptomycin (100×)	Yeasen	Cat# 60162ES76
phorbol 12-myristate 13-acetate (PMA)	Sigma	Cat# P1585
IPTG (Isopropyl-β-D-Thiogalactopyranoside)	Solarbio	Cat# I8070
Ni-NTA Agarose	Qiagen	Cat# 30210
16:0 PA	Avanti	Cat# 830855P
16:0 PS	Avanti	Cat# 840037P
Cholesterol	Beyotime	Cat# ST1155
MCC950	Sigma	Cat# PZ0280
Ac-YVAD-CMK	Sigma	Cat# SML0429
Necrosulfonamide (NSA)	Selleck	Cat# S8251
BAPTA-AM	Selleck	Cat# S7534
RIPA Lysis buffer	Sangon	Cat# C500005

(*Continued on next page*)

Continued

REAGENT or RESOURCE	SOURCE	IDENTIFIER
Potassium chloride (KCl)	Sinopharm	Cat# 10016318
2216E-dNaCl medium	This paper	N/A
Critical commercial assays		
CytoTox 96® Non-Radioactive Cytotoxicity Assay kit	Promega	Cat# G1780
Human IL-1β ELISA KIT	Solarbio	Cat# SEKH-0002
Human IL-18 ELISA KIT	Solarbio	Cat# SEKH-0028
DiO	Solarbio	Cat# D5840
DAPI	Sangon	Cat# E607303
Sparkjade ECL Plus	Shandong Sparkjade Biotechnology Co., Ltd.	Cat# ED0016
Membrane Lipid Strips™	Echelon Biosciences Inc	Cat# P-6002
Deposited data		
V13 genome sequence	NCBI	[GenBank]: [CP098021, CP098022]
Experimental models: Cell lines		
THP-1 cells	Cell Resource Center, IBMS, CAMS/PUMC	1101HUM-PUMC000057
NLRP3-KD THP-1 Cells	Invivogen	Cat# thp-dnlp
Casp1-KD THP-1 cells	Invivogen	Cat# thp-dcasp1
GSDMD-KO THP-1 cells	Zhao et al.[54]	N/A
ASC-KO THP-1 cells	This paper	N/A
Oligonucleotides		
gRNA targeting the sequence: ASC, 5'- GCTGGAGAACCTGACCGCCG-3'	This paper	N/A
Primers for VFH and δVFH, see Table S2	This paper	N/A
Recombinant DNA		
pDM4	Li et al.[58]	N/A
Escherichia coli SM10	Li et al.[58]	N/A
pBT3	Zhang et al.[59]	N/A
pET28a-SUMO	Ma et al.[60]	N/A

RESOURCE AVAILABILITY

Lead contact

Further information and requests for resources and reagents should be directed to the lead contact, Li Sun (lsun@qdio.ac.cn).

Materials availability

This study did not create new unique reagents. Requests for materials listed in key resources table should be directed to the lead contact.

Data and code availability

- The genome sequence of V13 has been deposited at NCBI and is publicly available as of the date of publication. Accession numbers are listed in the key resources table.
- This paper does not report original code.
- Any additional information required to reanalyze the data reported in this paper is available from the lead contact upon request.

EXPERIMENTAL MODEL AND STUDY PARTICIPANT DETAIL

Animals

Healthy turbots (average 15 g) were purchased from a local farm in Qingdao, Shandong Province, China. The fish were maintained at 20°C in aerated seawater. Live animal experiments were approved by the Ethics Committee of Institute of Oceanology, Chinese Academy of Sciences.

Cells and bacteria

The information of THP-1 cells and the gene knockout/knockdown cells were described in the key resources table. The cells were cultured in RPMI 1640 medium containing 10% fetal bovine serum and 1% antibiotic (penicillin and streptomycin) at 37°C in a cell incubator containing 5% CO_2. Unless otherwise specified, V13 and its mutants were cultured in 2216E medium at 28°C.

METHOD DETAILS

Bacterial culture and observation

Strain V13 was isolated from the deep sea water in Okinawa Trough (127°04'29.587"E, 27°16'02.831"N, depth 1587 m). The isolation was performed as reported previously.[32] Briefly, the seawater was spread on 2216E agar plates, and the plates were incubated at 28°C until the emergence of colonies. Bacteria were screened based on shape, size, color, and opacity. Sixty selected bacterial isolates were obtained and subjected to 16S rRNA sequence analysis, which identified 27 *Bacillus* spp., 7 *Alteromonas* spp., 4 *Gallaecimonas* spp., 4 *Aestuariibacter* spp., and one *Vibrio* spp. The Vibrio isolate proved to be *V. fluvialis* and was named V13. For morphology observation, the bacterial cells were re-suspended in ddH_2O and fixed with glutaraldehyde. After dehydrating with acetone, the cells were observed with a transmission electron microscope (TEM) (JEM-2100, Hitachi, Japan). For growth analysis, V13 was cultured in 2216E medium with different pH (5–10) and temperature (5°C–45°C) for 24 h or 48 h and measured for OD_{600} every 2 h. To examine the effect of NaCl on V13 growth, the marine broths that contained 0–10% (w/v) final NaCl were prepared according to the formula of 2216E-dNaCl Liquid Medium (peptone 5 g/L, yeast 1 g/L, Fe-$C_6H_5O_7$ 1 g/L, MgCl 5.98 g/L, Na_2SO_4 3.24 g/L, $CaCl_2$ 1.8 g/L, KCl 0.55 g/L, Na_2CO_3 0.16 g/L, KBr 0.08 g/L, $SrCl_2$ 0.034 g/L, H_3BO_3 0.022 g/L, $Na_2O \cdot nSiO_2$ 0.004 g/L, NaF 0.0024 g/L, NH_4NO_3 0.0016 g/L, and Na_2HPO_4 0.008 g/L), and V13 growth in these broths was determined.[53] The motility of V13 was determined as reported previously.[31] Briefly, V13 was cultured in 2216E medium to an OD_{600} of 0.8. The cells were collected by centrifugation and resuspended in PBS. Ten microliters of cell suspension were spotted on a filter disc placed in 2216E plate containing 0.3% (w/v) or 1.5% (w/v) agar. The plates were incubated at 28°C for 48 h, and bacterial growth was observed.

Cell culture

THP-1 cells and THP-1 cells with knockdown of Casp1 (Casp1-KD) and NLRP3 (NLRP3-KD) knockdown were purchased from the National Infrastructure of Cell Line Resource (China) and InvivoGen (France). THP-1 cells with GSDMD knockout (GSDMD-KO) were previously generated in our lab.[54] THP-1 cells with ASC knockout (ASC-KO) were created similarly, with the gRNA targeting the sequence of 5'- GCTGGAGAACC TGACCGCCG-3'. The ASC-KO knockout cells were verified by Western blot with antibody against human ASC (A11433, ABclonal) (Figure S6). All cell lines were cultured in RPMI1640 medium containing 10% fetal bovine serum and 1% penicillin and streptomycin (60162, Yeasen) at 37°C in a cell incubator containing 5% CO_2. All THP-1 cells used in this study were differentiated into macrophages by using phorbol 12-myristate 13-acetate (PMA) (P1585, Sigma) as reported previously.[42]

Genome sequencing and unique gene analysis

Total DNA of *V. fluvialis* V13 was prepared using the TIANamp Bacteria DNA Kit (DP302, TIANGEN), and genome sequencing was carried out as reported previously.[32] The genomes of V13 and ATCC 33809 were aligned using MUMmer and LASTZ tools. The unique gene were identified with OrthoMCL[55] and diamond.[56] The unique genes were subsequently annotated against NCBI non-redundant protein sequence (Nr) database, Kyoto Encyclopedia of Genes and Genomes (KEGG), Gene Ontology (GO), and Cluster of Orthologous Groups of proteins (COG) databases. The genome sequence of V13 was uploaded to NCBI (Gennamk: CP098021 and CP098022).

In vivo bacterial infection

In vivo infection was performed as reported previously.[57] Briefly, turbots were injected intramuscularly with V13 at the dose of 1×10^5, 3×10^5, or 1×10^6 CFU/g, and monitored for mortality for 7 days. For all infections, the control groups were injected with PBS. The median lethal dose (LD_{50}) was determined as reported previously.[38] To determine bacterial dissemination in fish tissues, the liver, spleen, kidney, and blood of turbot (five fish/time point) were sampled at 12, 18, and 24 h post-infection (hpi). The tissues were homogenized in PBS, and bacterial numbers in the homogenates were determined by plate count as reported previously.[59]

Construction of V13 mutants and complementary strains

V13 mutants were constructed using overlapping to construct V13ΔVFH, overlapping PCR was performed as reported previously.[58] Briefly, a 2126 bp section of VFH was deleted by overlap PCR first with the primer pair VFH-F1/R1 and then with the primer pair VFH-F2/R2, followed by the fusion PCR with the primer pair F1/R. The final PCR product was inserted into the suicide plasmid pDM4 at the *Xba*I and *Sal*I sites. The recombinant plasmid was introduced into *E. coli* SM10 via transformation. The transformants were conjugated with V13, and the conjugants were selected for sucrose resistance and chloramphenicol sensitivity as reported previously.[58] The resulting V13ΔVFH was verified for VFH in-frame deletion by PCR with the primer pair VFH-Fc/Rc. V13ΔδVFH was constructed as above, except that the first, second, and fusion PCR were performed with the primer pairs δVFH-F1/R1, δVFH-F2/R2, and δVFH-Fc/Rc, respectively. To construct the complementary strains V13ΔVFH/VFH, V13ΔδVFH/δVFH and V13ΔVFHΔδVFH/δVFH, the coding sequences of VFH and δVFH were amplified with the primer pairs VFH-F/R and δVFH-F/R, respectively. The PCR products were inserted into the EcoR V site of pBT3,[59] and the recombinant plasmids were introduced into V13ΔVFH, V13ΔδVFH and V13ΔVFHΔδVFH by electroporation. All PCR primers are listed in Table S4.

Purification of recombinant δVFH

The sequence of δVFH was amplified by PCR using the primers δVFH-F/R (Table S4). The PCR product was inserted into the plasmid pET28a-SUMO[60] at the *BamH1* and *XhoI* sites using ClonExpress II One Step Cloning Kit (C112, Vazyme). The recombinant plasmid was introduced into *Escherichia coli* BL21 (DE3) by transformation. The transformant was cultured in LB medium at 37°C to an OD_{600} of 0.5. IPTG (Isopropyl-β-D-Thiogalactopyranoside) was added to the culture at a final concentration of 0.1 mM. The culture was continued at 16°C for 15 h with shaking (100 rpm). The bacteria were then collected by centrifugation and ultrasonically broken. The recombinant protein was purified with nickel-nitrilotriacetic acid (Ni-NTA) columns as described previously.[61] The purified protein was dialyzed four times with PBS (6 h/time). The proteins were separated in 12% SurePAGE gels (M00667, GenScript) and stained with Coomassie blue (Figure S7). The control protein SUMO were previously purified in our lab.[62]

The cytotoxic effects of V13 variants and δVFH

The cytotoxicity assay was performed as reported previously.[42] Briefly, the PMA-pretreated THP-1 cells were incubated with V13 or δVFH at different concentrations (15.625–1000 nM). In the case where a specific inhibitor was used, the cells were pretreated with the inhibitor for 1 h and then treated with V13 or δVFH as above. The inhibitors included MCC950 (50 μM) (PZ0280, Sigma), Nec-1s (50 μM) (S8641, Selleck), Z-DEVD-FMK (50 μM) (S7312, Selleck), Ac-YVAD-CMK (50 μM) (SML0429, Sigma), NSA (20 μM) (S8251, Selleck), and BAPTA-AM (50 μM) (S7534, Selleck) targeting NLRP3, RIPK1, caspase 3, caspase 1, GSDMD, and Ca^{2+}, respectively. After treatment, the cells were observed with a microscope (Ti-S/L100, Nikon, Japan), and lactate dehydrogenase (LDH) release was measured with the CytoTox 96 Non-Radioactive Cytotoxicity Assay kit (G1780, Promega) according to the manufacturer's instruction. Briefly, the supernatant of the cells was transferred to a 96-well plate. An equal volume of CytoTox 96 Reagent was added to each well. The plate was incubated for 30 min at room temperature. Stop Solution was then added to the plate, and absorbance at 490 nm was determined with a microplate reader (Synergy H1, BioTek, USA).

Hemolysis assay

V13 variants were cultured in Marine 2216E broth to an OD_{600} of 0.8. The bacterial cells were collected by centrifugation at 8000*g* and washed three times with PBS. The cells were resuspended in PBS to 10^8 CFU/mL. Ten microliters of bacterial cell suspensions, recombinant hemolysins (VFH and δVFH), 2% Triton X-100 (positive control), and PBS (negative control) were dropped into filter discs in a 2216E agar plate containing 5% sheep blood. The plate was incubated at 28°C for 24 h and then observed for hemolysis.

Cytokine production analysis

IL-1β and IL-18 release from THP-1 cells was measured using human IL-1β and IL-18 ELISA kits (SEKH-0002/0028, Solarbio), respectively, according to the manufacturer's instructions.

Immunoblot

Western blot was performed as reported previously.[42] Briefly, the cells were lysed using RIPA Lysis buffer (C500005, Sangon), and the proteins were subjected to SDS-PAGE using 12% polyacrylamide gel (GenScript). The separated proteins were transferred to PVDF membranes. After blocking with 5% skimmed milk at room temperature for 1 h, the membranes were washed 3 times with TBST (TBS with 0.1% Tween 20) and treated with different antibodies against caspase 1 (3866T, Cell Signaling), GSDMD (69469S, Cell Signaling), His-tag (AE086, ABclonal), DnaK (cusabio), or actin (8226, abcam) for 1 h. The membranes were then treated with HRP-conjugated secondary antibody, and the proteins were detected with a Sparkjade ECL plus (ED0016, Shandong Sparkjade Biotechnology). To analyze the secretion of δVFH, V13, V13ΔδVFH, and V13ΔδVFH/δVFH were cultured in Opti-MEM to an OD_{600} of 0.8. The bacterial cultures were centrifuged (8000g, 3 min). The supernatants were collected and concentrated using Ultra Centrifugal Filter (UFC801096, Millipore). The cell pellets were resuspended in PBS and lysed by sonication. The supernatants and cell lysates were subjected to Western blot as above.

δVFH binding to cells and lipids

The binding of δVFH to cells and lipids was performed as reported previously.[42] THP-1 cells were transferred to glass-bottomed dishes (801001, NEST Biotechnology) and incubated overnight. The cells were stimulated with PBS, δVFH or SUMO (control) for 1 h, and then washed three times with PBS and fixed with 4% paraformaldehyde at room temperature for 15 min, followed by blocking in 5% BSA in PBST (PBS with 0.1% Tween 20) for 1 h. The cells were incubated with DyLights650 Anti-6×His antibody (1: 200 dilution) (ab117504, abcam) for 1 h at room temperature, followed by washing with PBST. The cells were incubated with DiO (10 μM) for 30 min and then washed with PBST. The cells were then incubated with DAPI (10 μg/mL) (E607303, Sangon) for 15 min and observed with confocal microscope (Carl Zeiss LSM900, Germany). The binding of δVFH (200 nM) to lipids was performed using Membrane Lipid Strips (P-6002, Echelon Biosciences Inc) as reported previously.[42]